ChemComm

Accepted Manuscript

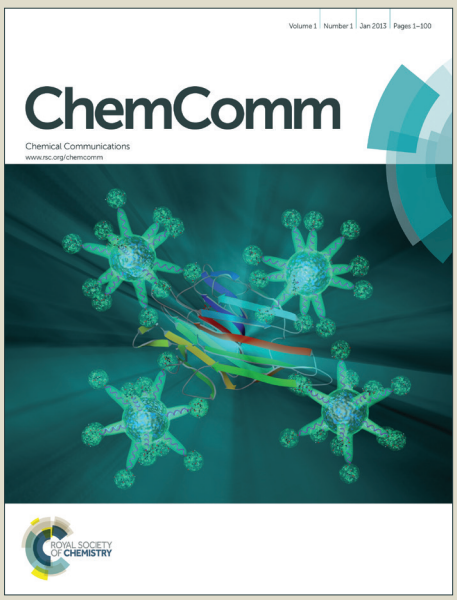

ROYAL SOCIETY OF CHEMISTRY

www.rsc.org/chemcomm

Journal Name

RSCPublishing

COMMUNICATION

Microwave *vs* solvothermal synthesis of hollow cobalt sulfide nanoprisms for electrocatalytic hydrogen evolution and supercapacitor

Cite this: DOI: 10.1039/x0xx00000x

Received ooth January 2012,
Accepted ooth January 2012

DOI: 10.1039/x0xx00000x

www.rsc.org/

Bo You,[†] Nan Jiang,[†] Meili Sheng and Yujie Sun*

Hollow cobalt sulfide nanoprisms obtained by a two-step microwave-assisted synthesis within 15 min exhibit higher hydrogen evolution catalytic activity and better specific capacitance than the counterpart prepared by a traditional solvothermal method.

Owing to the earth abundance and rich electrochemical properties, 1st-row transition metal sulfides (TMSs) have attracted significant attention for a variety of applications, including water splitting catalysis, solar cells, electrochemical sensors, Li-ion batteries, supercapacitors, thermoelectric devices, and memory devices.[1] For example, our group reported that electrodeposited cobalt and nickel sulfides exhibited excellent activity and robust stability towards hydrogen evolution reaction (HER) in aqueous media with a wide range of pH.[2] Although electrodeposition is a facile approach to obtain various TMSs for HER catalysis, its requirement of a conductive substrate as the working electrode might limit its application. For instance, it is not convenient to coat semiconductors and non-conductive substrates with TMSs via electrodeposition. Furthermore, the true potential of TMSs may be realized by introducing tailed nanoarchitecture with high specific surface area at lost-cost to achieve more advanced usability, including HER catalysis and supercapacitor.[3]

Resulting from the unique features of low density, high surface-to-volume ratio, kinetically favourable open structure and large void space fraction, hollow nanostructure has triggered tremendous research efforts for a myriad of applications, such as catalysis, drug delivery, and energy storage and conversion systems.[4] To date, numerous novel strategies have been developed in synthesizing hollow-structured materials.[4] Specifically, the approach based on the Kirkendall effect is very powerful and has been well developed.[4] For instance, Alivisatos's group used the Kirkendall effect to successfully synthesize hollow CoS.[5a] Lou et al reported a similar hydrothermal method to form hetero-structured $BiVO_4/Bi_2S_3$ hollow discoids within 18 h.[5b] However, despite these advances, hydrothermal or solvothermal synthesis of TMSs is typically time-consuming (usually several hours to days), and require high temperature/pressure conditions. Therefore it is highly desirable to explore alternative approaches of high efficiency and low energy cost to prepare hollow TMSs with advanced properties for multiple applications.

Herein, we demonstrate a facile two-step microwave-assisted synthetic route to obtain hollow cobalt sulfide nanoprisms (MW-CoS) within 15 min. Compared with the traditional solvothermal method, the microwave-assisted preparation is more effective in many facets, which has been proved to be more environmentally friendly and energy efficient.[6] More importantly, the resulting MW-CoS show higher catalytic activity for the hydrogen evolution reaction and improved specific capacitance compared to the counterpart (ST-CoS) prepared by a traditional time-consuming solvothermal approach. The overall synthetic procedure for MW-CoS is illustrated in Scheme 1 (for more synthetic details, see ESI†). The precursors of cobalt acetate hydroxide nanoprisms were firstly prepared by microwave irritation at 85 °C for 10 min, which were subsequently transferred to hollow cobalt sulfide in the presence of a sulfur source (thioacetamide, TAA) at 120 °C within 5 min due to the Kirkendall effect.[4a,e]

The morphology and microstructure of the as-prepared cobalt acetate hydroxide precursors (CAHs) after the first-step microwave treatment were characterized by scanning electron microscopy (SEM) and transmission electron microscopy (TEM). Fig. S1a shows the typical prism-like nanostructure of CAHs. The high-magnified SEM images (Fig. S1a, inset) reveal that each tetragonal nanoprism has a rather smooth surface. TEM images of highly dispersed CAHs reveal their solid and dense nature (Fig. S1b). The

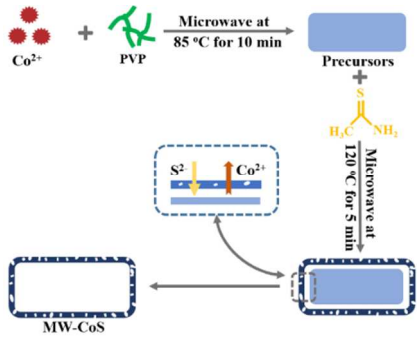

Scheme 1 Schematic route for the preparation of MW-CoS.

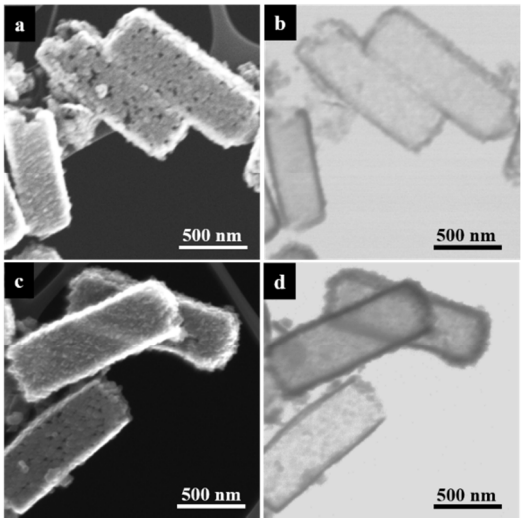

Fig. 1 SEM images of MW-CoS (a) and ST-CoS (c) and TEM images of MW-CoS (b) and ST-CoS (d).

phase composition of CAHs investigated by X-ray diffraction (XRD) could be assigned to a tetragonal cobalt acetate hydroxide phase (Fig. S2a, JCPDS card No. 22-0582). After the second-step microwave-assisted sulfurization treatment in a TAA solution, the resulting MW-CoS mostly inherited the overall nanoprism morphology of the mother CAHs and the surface became relatively rough and porous, as shown in the SEM images (Fig. 1a, more images available in Fig. S1). In some cases, several broken nanoprisms could be observed, implying the formation of hollow nanostructure. The TEM images further verify this conclusion. As shown in Fig. 1b, the sharp contrast between the centre and the edge of MW-CoS clearly demonstrates their hollow configuration with a shell thickness of ~30 nm. For comparison, a control sample (ST-CoS) using the same precursor and sulphur source was prepared solvothermally, where the reaction time was extended to 6 h at 120 ^{o}C. Similar hollow prism-like nanostructure of the resulting ST-CoS can be observed from the SEM and TEM images (Fig. 1c and d and Fig. S1). The only morphology difference between ST-CoS and MW-CoS is that MW-CoS possess rougher surface, implying higher porosity and hence larger specific surface area. The XRD patterns of MW-CoS and ST-CoS indicate the formation of hexagonal phase of CoS (Fig. S2, JCPDS card No. 65-8977). EDX results further confirmed the Co/S ratio close to 1 in both CoS samples (Fig. S3). In addition, the Co 2p and S 2p signal of XPS analysis (Fig. S4) are consistent with 2+ and 2− oxidation states of Co and S, respectively, for both MW-CoS and ST-CoS.[7]

In order to further validate our speculation, the porosity features of MW-CoS and ST-CoS were analysed by nitrogen adsorption-desorption measurements. As plotted in Fig. 2a, MW-CoS and ST-CoS both exhibit a type-III isotherm with a sharp capillary condensation step in the relative pressure (P/P_0) range from 0.9 to 1.0 and a H_3-type hysteresis loop, implying the presence of relatively large macropores and mesopores in the frameworks.[8] The H_3-type hysteresis loop is attributed to the hollow cavity space.[4d] Clearly, the adsorption of MW-CoS is higher than that of ST-CoS, indicating its higher specific surface area. The pore size distribution curves calculated from the adsorption branch of the isotherms resulted the primary pores of 4.8 and 2.2 nm for MW-CoS and ST-CoS respectively (Fig. 2b).[18] On the basis of the standard Brunauer−Emmett−Teller (BET) method and the BJH model, the specific surface area and total pore volume of MW-CoS were calculated to be 30.1 m^2 g^{-1} and 0.52 cm^3 g^{-1}, respectively, higher than those of ST-CoS (specific surface area of 27.5 m^2 g^{-1} and total pore volume of 0.16 cm^3 g^{-1}). Such higher specific surface area and larger pore volume in association with higher porosity are expected to show higher performance when MW-CoS are applied to HER catalysis and supercapacitor.

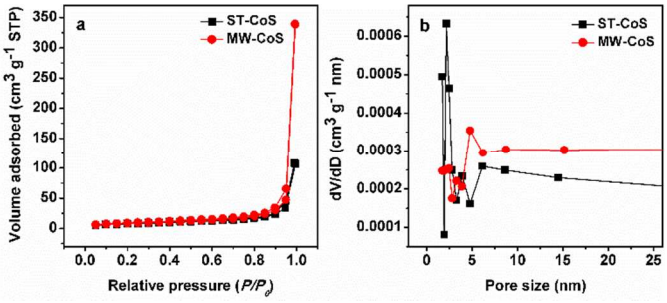

Fig. 2 (a) N_2 sorption isotherms and (b) pore size distribution curves of ST-CoS and MW-CoS.

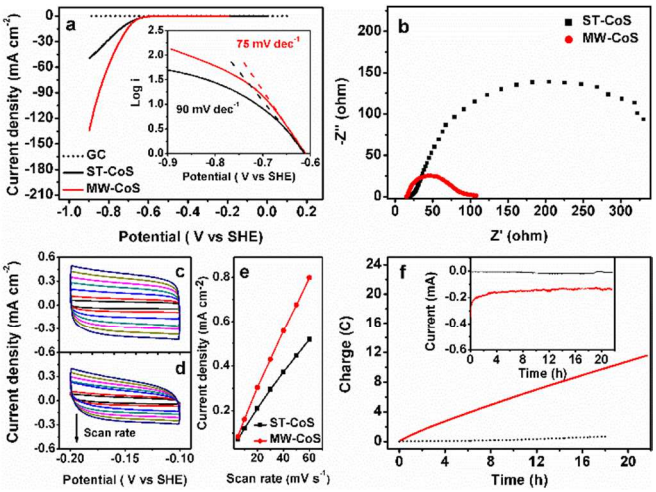

Fig. 3 (a) Polarization curves of GC, ST-CoS and MW-CoS in 1.0 M phosphate buffer of pH 7 at 2 mV s^{-1} and 2000 rpm. (b) EIS of ST-CoS and MW-CoS measured at -650 mV vs SHE. Cyclic voltammograms (CVs) of MW-CoS (c) and ST-CoS (d). (e) Scan rate dependence of the current densities of ST-CoS and MW-CoS at –0.15 V vs SHE. (f) Long-term controlled potential electrolysis of MW-CoS and blank electrode (dash lines) in 1.0 M phosphate buffer of pH 7 at –0.650 V vs. SHE. The insets in (a) and (f) are Tafel plots of MW-CoS and ST-Cos and the corresponding current change over time during electrolysis, respectively.

We first evaluated the catalytic HER activities of MW-CoS and ST-CoS in N_2-saturated pH 7 phosphate buffer via linear sweep voltammogram (LSV) on a rotating disk electrode (RDE) at 2000 rpm. The scan rate was set at 2 mV s^{-1} to minimize capacitive current (see details in ESI). As shown in Fig. 3a, the blank glassy carbon RDE (GC) possesses negligible HER catalytic activity between 0 to -0.9 V vs standard hydrogen electrode (SHE). In sharp contrast, rapid cathodic current rise was observed for both of MW-CoS and ST-CoS samples when the potential was scanned beyond -0.6 V vs SHE, accompanied with rigorous formation of hydrogen bubbles on the RDE surface. Notably, the overpotentials that required to drive cathodic current densities of 1, 10 and 50 mA cm^{-2} for MW-CoS is 198, 275, and 373 mV, respectively, which are significantly smaller than those of ST-CoS (201, 298 and 486 mV) and compare favourably with the performance of other earth-abundant HER catalysts at pH 7 (Table S1). Moreover, the corresponding Tafel slope of MW-CoS (75 mV dec^{-1}) is lower than that of ST-CoS (90 mV dec^{-1}), suggesting their better HER catalytic kinetics (Fig. 3a inset). Also, the semicircular diameter in the electric impedance

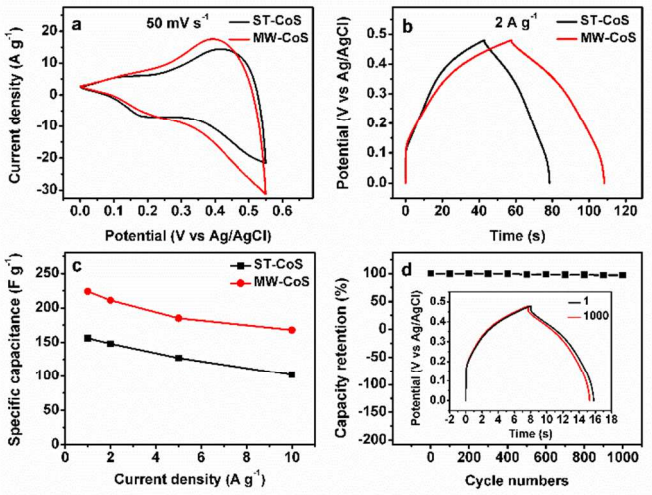

Fig. 4 (a) Cyclic voltammetry and (b) galvanostatic charge/discharge curves of ST-CoS and MW-CoS. (c) The variation of specific capacitances with current densities for ST-CoS and MW-CoS. (d) Capacity retention versus cycle numbers for MW-CoS at the current density of 10 A g^{-1}. The inset in (d) shows the galvanostatic charge-discharge curves of MW-CoS at the 1st and 1000th.

spectrum (EIS) for MW-CoS is much smaller than that for ST-CoS due to smaller contact and charge transfer impedance (Fig. 3b). To further estimate the effective surface area, the electrochemical double-layer capacitance was evaluated by cyclic voltammetry at non-Faradaic potentials of -0.1 to -0.2 V vs SHE (Fig. 3c and d). As well known, the effective surface area of materials of similar composition is proportional to its capacitance, which can be derived from the slope of the linear relationship between current density and scan rate.[2b,9] Fig. 3e clearly demonstrates that the slop of MW-CoS is larger than that of ST-CoS, suggesting the microwave-assisted synthesis for hollow cobalt sulfide is more effective in enlarging the catalytically active surface area in comparison to the conventional solvothermal method. These results are also consistent with the larger pore size and increased surface area of MW-CoS measured by the BET method.

Next, we evaluated the long-term stability of MW-CoS as shown in Fig. 3f, which presents a nearly linear charge accumulation with a steady current over 21h, implying robust durability of MW-CoS as HER catalysts. Hydrogen quantification via gas chromatography confirmed their nearly 100% Faradaic efficiency. Overall, the improved catalytic HER activity of MW-CoS compared to HT-CoS is ascribed to the larger porosities and higher specific surface area of the former, which promote rapid mass transport and accessibility of catalytic active sites.[2] In addition, the MW-CoS also exhibited very efficient HER activity and excellent stability in strong alkaline electrolyte (1.0 M KOH, Fig. S5), which allows its compatible integration with oxygen evolution catalysts for overall water splitting catalysis.

The supercapacitors based on MW-CoS and ST-CoS were measured to further highlight the superiority of microwave-assisted synthesis for hollow cobalt sulfide. The tests were carried out with a three-electrode cell employing MW-CoS and ST-CoS coated glassy carbon electrodes as the working electrodes in 1.0 M KOH solution (for experimental details, see ESI†). As depicted in Fig. 4a and Fig. S6, the cyclic voltammetry (CV) curves of both MW-CoS and ST-CoS electrodes show a box-like shape, indicating the coexistence of an electric double-layer capacitance (EDL) and pseudocapacitance related to reversible Faradaic reactions of cobalt sulfide.[4b,8c] Apparently, the CVs of MW-CoS exhibit a higher current density than those of ST-CoS at all scan rates, representing a higher capacitance.[8] The galvanostatic (GV) discharge time of MW-CoS is also significantly greater in comparison to that of ST-CoS (Fig. 4b and Fig. S7). It's well known that the specific capacitance is proportional to the discharge time under the GV curve. These data unambiguously prove that MW-CoS afford larger charge capacity. More importantly, the specific capacitance vs. current density, as summarized in Fig. 4c, indicates that MW-CoS result in a greatly improved capacitance and enhanced rate capability compared to ST-CoS. For example, the highest specific capacitance of MW-CoS is 224 F g^{-1} at a current density of 1.0 A g^{-1}, which is substantially higher than that of ST-CoS (156 F g^{-1}) and other reported cobalt sulfide under similar conditions.[10] Additionally, a high specific capacitance of 168 F g^{-1} can be retained even when the current density increases by as much as 10 times (to 10 A g^{-1}), confirming its good rate capability. These results highlight the positive structure effect of MW-CoS achieved by the microwave synthesis. The larger pores as well as higher specific surface area could buffer electrolytes to reduce ion transport resistance and ion diffusion distance for high-rate supercapacitors and also enhance the charge storage for high specific capacitance.[8] The electric impedance spectroscopy (EIS) results also supported this speculation (Fig. S8).

Cycling performance is another key factor in determining the quality of supercapacitor electrodes for many practical applications. A long time galvanostatic charge/discharge cycling for up to 1000 cycles was performed on the MW-CoS electrodes. The results, shown in Fig. 4d, indicate that 97% of the initial capacitance has been retained and the shape of charge-discharge curves after 1000 cycles matches the first cycle very well (Fig. 4d inset). The superior performance of MW-CoS should be attributed to the excellent kinetic properties of their large porosity which facilitate the movement of electrolyte. Further increased capacitance could be naturally anticipated if MW-CoS is decorated with conductive carbon materials of high specific surface area,[11] which is under current investigation.

In summary, we have successfully synthesized hollow cobalt sulfide nanoprisms through a facile two-step microwave-assisted synthetic route within 15 min (MW-CoS). Compared with the traditional solvothermal method, this microwave-assisted approach is very time- and energy-efficient. More importantly, the resulting MW-CoS present higher electrocatalytic activity for the hydrogen evolution reaction (overpotential of 373 mV vs 486 mV to reach a current density of 50 mA cm^{-2}) and improved specific capacitance (43 % improvement) compared to the counterpart, rendering them very promising candidates for advanced electrocatalysis and energy storage.

This work was supported by the Utah State University (USU). N.J. acknowledges the Governor's Energy Leadership Scholars grant program of the State of Utah. Y.S. acknowledges the financial support from the Principle Energy Issues Program of the State of Utah. SEM and TEM measurement were conducted by FenAnn Shen at the Microscopy Core Facility of USU. This work also made use of the Surface Analysis and Nanoscale Imaging group at the University of Utah, sponsored by the College of Engineering, Health Sciences Center, Office of the Vice President for Research, and the Utah Science Technology and Research (USTAR) Initiative of the State of Utah.

Notes and references

[a] Department of Chemistry and Biochemistry, Utah State University, Logan, Utah 84322, USA. E-mail: yujie.sun@usu.edu; Fax: +1-435-797-3390; Tel: +1-435-797-7608

† These authors contributed equally

Electronic Supplementary Information (ESI) available: Experimental details, SEM and TEM images, galvanostatic charge/discharge curves, EIS for the samples and additional table. See DOI: 10.1039/c000000x/

1 (a) K. Roy, M. Padmanabhan, S. Goswami, T. P. Sai, G, Ramalingam, S. Raghavan and A. Ghosh, *Nat. Nanotech*., 2013, **8**, 826; (b) M. R. Gao, Y. F. Xu, J. Jiang and S. H. Yu, *Chem. Soc. Rev*., 2013, **42**, 2986; (c) T. F. Jaramillo, K. P. Jorgensen, J. Bonde, H. H. Nielsen, S. Horch and I. Chorkendorff, *Science*, 2007, **317**, 100; (d) W. Chen, C. Xia, H. N. Alshareef, *ACS Nano*, 2014, **8**, 9531; (e) Y. Zheng, Y. Jiao, M. Jaroniec and S. Z. Qiao, *Angew. Chem. Int. Ed*., 2015, **54**, 52.

2 (a) Y. J. Sun, C. Liu, D. C. Grauer, J. Yano, J. R. Long, P. D. Yang and C. J. Chang, *J. Am. Chem. Soc*., 2013, **135**, 17699; (b) N. Jiang, L. Bogoev, M. Popova, S. Gul, J. Yano and Y. J. Sun, *J. Mater. Chem. A*, 2014, **2**, 19407.

3 (a) J. D. Benck, T. R. Hellstern, J. Kibsgaard, P. Chakthranont and T. F. Jaramillo, *ACS Catal*., 2014, **4**, 3957; (b) J. Kibsgarrd, Z. Chen, B. N. Reinecke, T. F. Jaramillo, *Nat. Mater*., 2012, **11**, 963.

4 (a) Y. D. Yin, R. M. Rioux, C. K. Erdonmez, S. Hughes, G. A. Somorjai and A. P. Alvisatos, *Science*, 2004, **304**, 711; (b) L. Yu, L. Zhang, H. B. Wu and X. W. Lou, *Angew. Chem. Int. Ed*., 2014, **53**, 3711; (c) W. Li, Y. H. Deng, Z. X. Wu, X. F. Qian, J. P. Yang, Y. Wang, D. Gu, F. Zhang, B. Tu and D. Y. Zhao, *J. Am. Chem. Soc*., 2011, **133**, 15830; (d) B. You, J. Yang, Y. Q. Sun and Q. D. Su, Chem. Commun., 2011, **47**, 12364; (e) W. S. Wang, M. Dahl and Y. D. Yin, *Chem. Mater*., 2013, **25**, 1179; (f) Y. D. Liu, J. Goebl and Y. D. Yin, *Chem. Soc. Rev*., 2013, **42**, 2610.

5 (a) Y. D. Yin, C. K. Erdonmez, A. Cabot, S. Hughes and A. P. Alivisatos, Adv. Funct. Mater., 2006, **16**, 1389; (b) X. H. Gao, H. B. Wu, L. X. Zheng, Y. J. Zhong, Y. Hu and X. W. Lou, *Angew. Chem. Int. Ed*., 2014, 53, 5917.

6 (a) H. J. Kitchen, S. R. Wallance, J. L. Kennedy, N. Tapia-Ruiz, L. Carassiti, A. Harrison, A. G. Whittaker, T. D. Drysdale, S. W. Kingman and D. H. Gregory, *Chem. Rev*., 2014, **114**, 1170; (b) M. Baghbanzadeh, L. Carbone, P. D. Cozzoli and C. O. Kappe, *Angew. Chem. Int. Ed*., 2011, **50**, 11312; (c) Y. J. Zhu and F. Chen, *Chem. Rev*., 2014, **114**, 6462; (d) H. Pang, C. Z. Wei, X. X. Li, G. C. Li, Y. H. Ma, S. J. Li, J. Chen and J. S. Zhang, *Sci. Rep*., 2014, **4**, 3577.

7 W. J. Dong, X. B. Wang, B. J. Li, L. N. Wang, B. Y. Chen, C. R. Li, X. Li, T. R. Zhang and Z. Shi, *Dalton Trans*., 2011, **40**, 243.

8 (a) B. You, L. L. Wang, N. Li and C. L. Zheng, *ChemElectroChem*, 2014, **1**, 772; (b) B. You, J. H. Jiang and S. J. Fan, *ACS Appl. Mater. Interfaces*, 2014, **6**, 15302; (c) B. You, P. Q. Yin and L. N. An, *Small*, 2014, **10**, 4352; (d) W. M. Du, Z. Q. Zhu, Y. B. Wang, J. N. Liu, W. J. Yang, X. F. Qian and H. Pang, *RSC Adv*., 2014, **4**, 6998.

9 T. Y. Ma, S. Dai, M. Jaroniec and S. Z. Qiao, *J. Am. Chem. Soc*., 2014, **136**, 13925.

10 (a) S. Amaresh, K. Karthikeyan, I. C. Jang and Y. S. Lee, *J. Mater. Chem. A*, 2014, **2**, 11099; (b) B. Wang, J. Park, D. W. Su, C. Y. Wang, H. Ahn and G. X. Wang, *J. Mater. Chem*., 2012, **22**, 15750.

11 W. M. Du, Z. Y. Wang, Z. Q. Zhu, S. Hu, X. Y. Zhu, Y. F. Shi, H. Pang and X. F. Qian, *J. Mater. Chem. A*, 2014, **2**, 9613.

